European Journal of Cardio-Thoracic Surgery 61 (2022) 1307–1315
https://doi.org/10.1093/ejcts/ezac016 Advance Access publication 25 January 2022

ORIGINAL ARTICLE

Cite this article as: Cvitkovic T, Bobylev D, Horke A, Avsar M, Beerbaum P, Martens A *et al.* 4D-flow cardiac magnetic resonance imaging after aortic root replacement with long-valved decellularized aortic homografts: comparison to valve-sparing aortic root replacement and healthy controls. Eur J Cardiothorac Surg 2022;61:1307–15.

4D-flow cardiac magnetic resonance imaging after aortic root replacement with long-valved decellularized aortic homografts: comparison to valve-sparing aortic root replacement and healthy controls

Tomislav Cvitkovic [a,*], Dmitry Bobylev[a], Alexander Horke [a], Murat Avsar[a], Philipp Beerbaum [c], Andreas Martens [a], Dietmar Böthig[a], Elena Petenà[a], Marcel Gutberlet[b], Frerk Hinnerk Beyer[b], Frank Wacker[b], Serghei Cebotari[a], Axel Haverich[a], Jens Vogel-Claussen[b], Samir Sarikouch [a] and Christoph Czerner[b]

[a] Department for Cardiothoracic, Transplant, and Vascular Surgery, Hannover Medical School, Hannover, Germany
[b] Institute for Diagnostic and Interventional Radiology, Hannover Medical School, Hannover, Germany
[c] Department for Pediatric Cardiology and Intensive Care, Hannover Medical School, Hannover, Germany

* Corresponding author. Department for Cardiothoracic, Transplant, and Vascular Surgery, Hannover Medical School, Carl-Neuberg-Str. 1, Hannover 30625, Germany. Tel: +49-511-532-9829; e-mail: cvitkovic.tomislav@mh-hannover.de (T. Cvitkovic).

Received 25 August 2021; received in revised form 29 November 2021; accepted 10 January 2022

Key question

Can long decellularized homografts restore normal blood flow in the ascending aorta?

Key finding(s)

Long decellularized aortic homografts exhibit near normal haemodynamic parameters, e.g. energy loss, 2.56 ± 2 years postoperatively.

Take-home message

Decellularized homografts are an additional surgical option in patients with aortic valve pathology and dilatation of the ascending aorta.

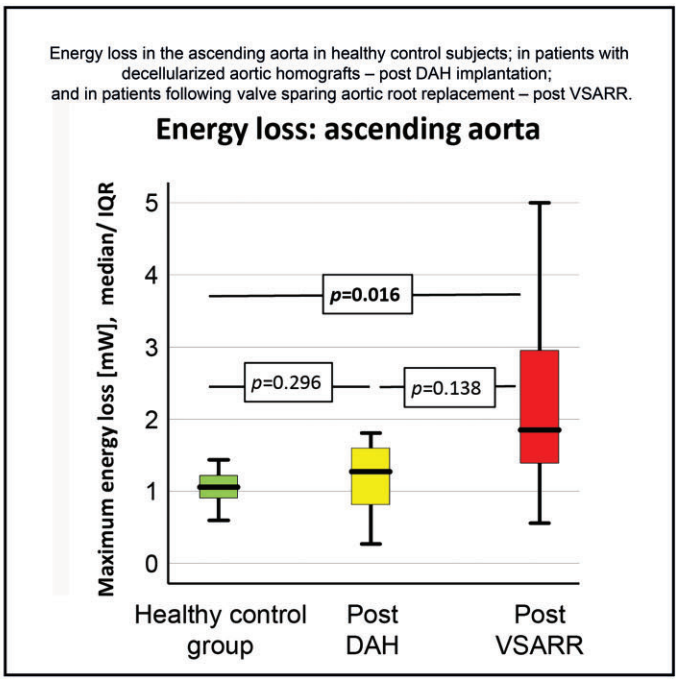

Abstract

OBJECTIVES: Long-valved decellularized aortic homografts (DAH) may be used in young patients to treat aortic valve disease associated with aortic root dilatation, thereby eliminating the need for prosthetic material and anticoagulation.

METHODS: Thirty-three male subjects in 3 equally sized cohorts were compared: patients following DAH implantation with a median age of 29 years [interquartile range (IQR) 27.5–37.5], patients post-valve-sparing aortic root replacement (VSARR), median 44 years (IQR 31.5–49) and healthy controls, median 33 years (IQR 28–40, $P = 0.228$). Time-resolved three-dimensional phase-contrast cardiac

magnetic resonance imaging was performed to assess maximum blood flow velocity, pulse wave velocity, mechanical energy loss (EL), wall shear stress and flow patterns (vorticity, eccentricity, helicity) in 5 different planes of the aorta.

RESULTS: The mean time between surgery and cardiovascular magnetic resonance was 2.56 ± 2.0 years in DAH vs 2.67 ± 2.1 in VSARR, $P = 0.500$. No significant differences in maximum velocity and pulse wave velocity were found between healthy controls and DAH across all planes. Velocity in the proximal aorta was significantly higher in VSARR (182.91 ± 53.91 cm/s, $P = 0.032$) compared with healthy controls. EL was significantly higher in VSARR in the proximal aorta with 1.85 mW (IQR 1.39–2.95) compared with healthy controls, 1.06 mW (0.91–1.22, $P = 0.016$), as well as in the entire thoracic aorta. In contrast, there was no significant EL in DAH in the proximal, 1.27 m/W (0.92–1.53, $P = 0.296$), as well as in the thoracic aorta, 7.7 m/W (5.25–9.90, $P = 0.114$), compared with healthy controls. There were no significant differences in wall shear stress parameters for all 5 regions of the thoracic aorta between the 3 groups. DAH patients, however, showed more vorticity, helicity and eccentricity in the ascending aorta compared with healthy controls ($P < 0.019$).

CONCLUSIONS: Decellularized long aortic homografts exhibit near to normal haemodynamic parameters 2.5 years postoperatively compared with healthy controls and VSARR.

Keywords: Aortic valve disease • Haemodynamics • 4D flow • Decellularized homograft • Aortic root replacement

ABBREVIATIONS

DAH	Decellularized aortic homografts
EL	Energy loss
IQR	Interquartile range
LVOT	Left ventricle outflow tract
PWV	Pulse wave velocity
VSARR	Valve-sparing aortic root replacement

INTRODUCTION

Limited surgical options are available for aortic valve pathology associated with ascending aortic dilatation. Mechanical and biological aortic valve prostheses in combination with vascular grafts are the most frequently used substitutes in clinical practice [1]. If there is a chance to preserve the aortic valve, valve-sparing aortic root replacement (VSARR) in combination with prosthetic aorta ascendens replacement has shown excellent long-term results [2].

Decellularized aortic homografts (DAH) present a new surgical option in aortic valve disease associated with aortic root dilatation, especially for young patients. DAH, including the implantation of long homografts, were introduced to the clinic over a decade ago and have shown good early results [3]. They eliminate the need for any prosthetic material and do not require long-term anticoagulation. In contrast to vascular prostheses, they are structurally almost identical to native aortic valves with lesser impact on haemodynamics. This is important as the physiology of the ascending aorta is complex: systolic expansion occurs at high speed and is directly influenced by peripheral blood pressure, and the diastolic function of the ascending aorta in addition is an important contributor to coronary blood flow. Systolic compliance and diastolic function appear to have a long-term impact on vascular and cardiac remodelling [4].

Four-dimensional flow cardiovascular magnetic resonance imaging (4D-flow CMR) allows for a comprehensive assessment of vessel morphology and function as well as blood haemodynamics. 4D-flow CMR facilitates the assessment of pulse wave velocity (PWV) as a marker for regional aortic stiffness [5–7], the visualization of complex blood flow patterns such as helicity, vorticity and eccentricity and the quantification of wall shear stress (WSS) [8]. 4D-flow CMR has already been used to evaluate effects of surgery on aortic geometry and compliance [9, 10]. Aortic arch PWV, for example has been shown to be closely related to the bioelastic properties of the aorta [11]. PWV propagation was significantly faster in the stiffened aorta leading to higher systolic pressures within the proximal aorta and an increased left ventricular load [12]. Aortic stiffness was shown to be an important direct predictor of all-cause and cardiovascular mortality [13–15].

In contrast to VSARR [16], data on blood flow haemodynamics in patients who underwent aortic root replacement with long DAH are lacking. The aim of this study therefore was to provide these data using 4D-flow CMR and to compare the results with a cohort of VSARR patients and healthy controls. We hypothesized that DAH patients would have similar aortic haemodynamics to healthy volunteers.

METHODS

Ethics statement

This prospective study was approved by the institutional ethics committee (Ethics Committee of the Medical School of Hannover, Germany, with EC No 7960_BOS_2018c) and written informed consent was obtained from all study participants.

Study population

Three study groups were analysed, healthy control subjects ($n = 11$), patients following DAH implantation ($n = 11$) and patients after VSARR ($n = 11$). Only males ≥18 years of age with no contraindications for magnetic resonance imaging, e.g. incompatible implants, and no significant aortic regurgitation were selected. The patient groups were matched in terms of the time interval between surgery and CMR during the inclusion process and echocardiographic data at discharge were available for all patients. Only patients, who had undergone surgery at our hospital between 2013 and 2019 and who were categorized in NYHA class I, postoperatively were included to avoid any confounding factors potentially caused by an impaired left ventricular function or suboptimal surgical results.

Severe aortic valve regurgitation was the indication in 10 of 11 VSARR patients and 1 patient had predominant stenosis. Aortic regurgitation was the indication in 4 DAH patients, 3 DAH patients had aortic stenosis and 4 patients had combined valvular pathology. There was no difference in preoperative left ventricular size and function {DAH 52.27 ± 8.87 mm LVED vs 52.45 ± 7.24 mm in VSARR, $P = 0.959$; DAH LV EF median 60%

[interquartile range (IQR) 55–70%] vs VSARR LV EF 60% (IQR 54–63%), $P = 0.748$}.

DAH patients significantly underwent more previous cardiac procedures (see Table 1). No additional left ventricle outflow tract (LVOT) procedures, e.g. subannular resections, Konno or other patch plasties, were performed during the DAH implantations or the VSARR procedures.

Surgical technique

In both patient groups, full median or upper mini hemisternotomy was performed and cold blood cardioplegia was used for myocardial protection during cardiopulmonary bypass. The coronary ostia were excised and reimplanted as buttons. Aortic valve homografts were provided by 2 tissue establishments (Deutsche Gesellschaft für Gewebetransplantation, Hannover and the European Homograft Bank, Brussels) and were processed for decellularization at Corlife oHG, Hannover, as described previously [3]. Following successful processing and subsequent release, the DAH were implanted using a full root technique. All DAH were long grafts, and distal anastomoses were performed typically 2–3 cm proximal to the Truncus brachiocephalicus using standard cardiopulmonary bypass without hypothermic circulatory arrest.

No additional prosthetic material was used in the DAH group.

VSARR was performed using a David I technique as described previously [2]. In all VSARR patients, a straight tube graft was used. The aortic sinuses were resected up to a rim of 5 mm of the aortic wall. The aortic annulus size was measured with Hegar dilators. We typically chose the vascular graft for aortic root replacement 2 mm bigger than the annulus size [2].

Magnetic resonance imaging

Magnetic resonance imaging was performed using a 1.5-T scanner (MAGNETOM Avanto; Siemens Healthineers GmbH, Erlangen, Germany). An eight-channel torso phased array coil was used for all sequences.

Morphological images were acquired for the planning of cardiac and 4D flow sequences.

Blood flow was evaluated with 4D phase-contrast imaging [17], which did not require contrast medium, in a sagittal oblique volume of the thoracic aorta. 4D flow imaging was conducted prospectively electrocardiography gated during free breathing with a respiratory navigator placed on the lung–liver interface. For more informations about our Magnetic resonance imaging please see Supplementary Material.

Image and data analyses

Phase-contrast and short axis cine images were analysed with CVI 42 version 5.11 (Circle Cardiovascular Imaging Inc., Calgary, Canada). Parameter nomenclature and calculation followed common standards [18].

4D flow images were corrected for eddy currents, Maxwell terms and aliasing. Flow calculations were analysed at 5 distinct locations at which the aorta was segmented in a cross-sectional plane: (1) at the level of the aortic valve, (2) in the proximal ascending aorta, (3) in the distal ascending aorta up to the first aortic arch vessel, (4) at the beginning of the descending aorta distal to the origin of the left subclavian artery, and (5) in the descending aorta at the level of the aortic valve.

Table 1: Characteristics and heart function in all 3 cohorts (healthy controls, decellularized aortic homografts, valve-sparing aortic root replacement)

Characteristics	Healthy controls ($n = 11$)	DAH ($n = 11$)	VSARR ($n = 11$)	P-omnibus
Age at follow-up (years), median (IQR)	32 (28–40)	29 (27.5–37.5)	44 (31.5–49)	0.228
Time interval between surgery and MRI (years), mean (SD)	n.a.	2.56 (2.0)	2.67 (2.1)	0.500[a]
Number of previous aortic valve operations	n.a.	7 (5 x AV repair, 2 x replacement)	1 (Ross procedure)	
Number of previous cardiac procedures	n.a.	9	3	**0.001**[a]
Diameter of the aortic valve (mm), mean (SD)	24.64 (1.75)	27.36 (2.54)	26.18 (2.23)	**0.023**[b]
Diameter of the aorta ascendens (mm), mean (SD)	29.27 (3.03)	31 (1,79)	30 (2.83)	0.307
BMI (kg/m^2), mean (SD)	25.6 (4.5)	24.6 (2.3)	25.3 (3.1)	0.822
BSA (Mosteller formula) (m^2), mean (SD)	2.0 (0.2)	2.0 (0.2)	2.1 (0.2)	0.945
Systolic blood pressure (mmHg), mean (SD)	120 (9)	118 (10)	120 (14)	0.819
Diastolic blood pressure (mmHg), mean (SD)	70 (11)	71 (9)	72 (10)	0.990
Heart rate (beats/min), mean (SD)	67 (9)	73 (12)	67 (10)	0.254
Height (cm), mean (SD)	180 (6)	182 (9)	182 (8)	0.765
Weight (kg), mean (SD)	82.5 (14.2)	81.5 (10.9)	83.9 (16.1)	0.991
LVCO by CMR (l/min/m^2), mean (SD)	3.97 (0.44)	4.31 (0.38)	4.26 (0.82)	0.337
LVEF (%), mean (SD)	66.54 (5.07)	68.27 (6.86)	63.18 (5.36)	0.141
LVEDV by BSA (kg/m^2), mean (SD)	89.91 (15.67)	86.73 (8.92)	103.41 (19.95)	**0.038**[c]
LVM by BSA (g/m^2), mean (SD)	65 (9)	81 (19)	81 (18)	0.052
LVSV by BSA (ml/m^2), median (IQR)	57 (55–61)	60 (56–62)	66 (58–70)	0.214

Mean and SD are for normally distributed factors and median and IQR are for no normal distribution.

[a]Mann–Whitney U-test.

[b]Healthy controls versus VSARR, P-value = 0.328; healthy controls versus DAH, P-value = 0.020; DAH versus VSARR, P-value = 0.650.

[c]Healthy controls versus VSARR, P-value = 0.081; healthy controls versus DAH, P-value = 0.602; DAH versus VSARR, P-value = 0.054.

Bold numbers delineate significant differences. AV: aortic valve; BMI: body mass index; BSA: body surface area; CMR: cardiovascular magnetic resonance imaging; DAH: decellularized aortic homografts; IQR: interquartile range; LVCO: left ventricular cardiac output; LVEF: left ventricular ejection fraction; LVM: left ventricular mass; LVSV: left ventricular stroke volume; MRI: magnetic resonance imaging; n.a.: not applicable; SD: standard deviation; VSARR: valve-sparing aortic root replacement.

Several parameters were derived from phase-contrast images: forward volume (ml), maximum velocity (cm/s) and PWV [19–21]. WSS describes the shear force of the flowing blood and the vessel wall [22]. In addition, energy loss (EL), i.e. viscous EL, was determined [23]. Overall, PWV was calculated for the whole thoracic aorta (from the aortic valve to descending aorta) and separately for the ascending aorta (from the aortic valve to distal ascending aorta). The maximum EL was evaluated for the whole thoracic aorta (from the aortic valve to descending aorta) and separately for the ascending aorta (from the aortic valve to distal ascending aorta) [23].

Aortic blood flow was visualized four-dimensionally with streamlines and pathlines to assess blood flow patterns. Vorticity and helicity were semi-quantitatively graded in 3 categories: 0 = none, 1 = moderate (≤360°), 2 = severe (>360°) [24, 25]. Eccentricity of flow was also semi-quantitatively graded in 3 categories: 0 = central flow (occupying the majority of the vessel lumen), 1 = mild eccentric flow (occupying two-thirds to one-third of the vessel) and 2 = marked eccentric flow (occupying one-third or less of the vessel) [24].

CMR images were analysed by a single observer, Christoph Czerner. Semi-quantitative grading of vorticity, helicity and eccentricity was conducted as a consensus read by Christoph Czerner and Frerk Hinnerk Beyer.

Statistical analysis

Metric data are shown as a mean with standard deviation or a median with IQR if not otherwise indicated. We tested for normality via the Shapiro–Wilk test. As the distribution was mostly non-normal, we applied Mann–Whitney *U* tests for the comparison of 2 cohorts and the Kruskal–Wallis one-way analysis of variance with Dunn's multiple comparisons test (control versus DAH, control versus VSARR, DAH versus VSARR) for comparison between all 3 cohorts. Family-wise *P*-value correction with the Benjamini–Hochberg procedure was applied to control for a false discovery rate in Dunn's multiple comparison tests. To compare the normally distributed aortic diameters, we first assessed their homogeneous variances (Levene) and, then, we used an ANOVA, followed by pairwise Bonferroni-corrected *post hoc* tests. The significance level was set to 5%. 95% confidence intervals were not adjusted for multiple comparisons and inferences drawn from them may not be reproducible.

RESULTS

Subject demographics

In total, $n = 33$ participants were included in the study. The median age was 32 years (IQR 28–40) for healthy controls ($n = 11$), 29 years (IQR 27.5–37.5) for DAH patients ($n = 11$) and 44 years (IQR 31.5–49) for VSARR patients ($n = 11$), with no statistically different variance (*P*-omnibus = 0.228).

The mean follow-up time of CMR analysis after surgery was 2.56 ± 2.0 years for DAH patients and 2.67 ± 2.1 years for VSARR patients ($P = 0.500$). There were no statistically significant differences found for age, body mass parameters and myocardial function across all study groups, as assessed by short axis volumetry.

Seven out of 11 DAH patients had a bicuspid aortic valve. All VSARR patients and all controls had tricuspid aortic valves. Seven DAH patients had undergone previous LVOT operations, and 1 VSARR patient had undergone a previous LVOT operation. In total, there were 9 previous cardiac operations in the DAH group and 3 in the VSARR group. Detailed characteristics of the 3 cohorts are given in Table 1.

Blood flow velocity, pulse wave velocity and energy loss

No statistically significant differences in maximal velocities were observed between DAH patients and the healthy control subjects. There was a significantly higher maximum blood flow velocity after VSARR (182.91 ± 53.9 cm/s) compared with the healthy control group (134.82 ± 18.7 cm/s, $P = 0.032$) at the level of the distal ascending aorta. The results showing the maximum blood flow velocity in analysis planes 1–5 are summarized in Fig. 1.

PWV did not differ significantly between the groups (Table 2). There was significantly increased EL at the level of the proximal ascending aorta in VSARR patients with a median of 1.85 mW (IQR 1.39–2.95) compared with the healthy control group (median 1.06 mW, IQR 0.91–1.22, $P = 0.019$). EL was also significantly increased for VSARR in the entire thoracic aorta (8.8 mW, IQR 6.8–14.55 compared with healthy control subjects 5 mW, IQR 3.25–5.7, $P = 0.009$).

There were no significant differences in maximum EL between the healthy control group and DAH patients for the ascending and thoracic aorta (Table 2).

Magnitudinal wall shear stress and blood flow patterns

There were no significant differences for magnitudinal WSS in all 5 analysed aortic planes between both patient groups and the healthy control group (Table 2 and Fig. 2a).

There was no significant difference in eccentricity, helicity and vorticity between VSARR patients and the healthy control group (Table 3). DAH patients in contrast showed significantly more disturbed blood flow in the proximal and distal ascending aorta,

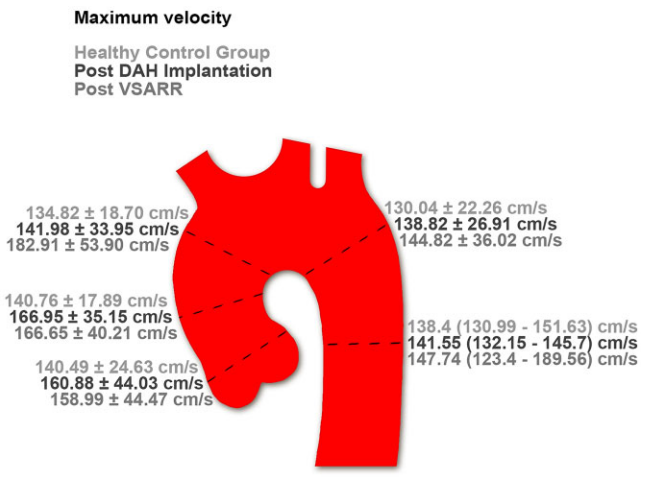

Figure 1: Maximal velocities in all 3 cohorts at 5 distinct locations at which the aorta was segmented in a cross-sectional plane. Upper values show the healthy controls, middle values decellularized aortic homograft and lower values show the results in valve-sparing aortic root replacement. Bold numbers delineate results of DAH patients.

Table 2: Maximal velocity, maximal energy loss, pulse wave velocity and magnitudinal wall shear stress in all 3 cohorts (healthy control, decellularized aortic homografts, valve-sparing aortic root replacement)

Variable	Location	Healthy controls ($n = 11$)	DAH ($n = 11$)	VSARR ($n = 11$)	*P*-omnibus	Healthy controls versus DAH, *P*-value	Healthy controls versus VSARR, *P*-value	DAH versus VSARR, *P*-value
MV (cm/s), mean (SD)	AV	140.49 (24.63)	160.88 (44.03)	158.99 (44.47)	0.586	0.585	0.585	0.947
MV (cm/s), mean (SD)	PAA	140.76 (17.89)	166.95 (35.15)	166.65 (40.21)	0.147	0.169	0.169	0.843
MV (cm/s), mean (SD)	DAA	134.82 (18.71)	141.98 (33.95)	182.91 (53.91)	0.026	0.581	**0.032**	0.067
MV (cm/s), mean (SD)	BDA	130.04 (22.26)	138.82 (26.91)	144.82 (36.02)	0.652	0.774	0.774	0.774
MV (cm/s), median (IQR)	DA	138.4 (130.99–151.63)	141.55 (132.15–145.71)	147.74 (123.4–189.56)	0.686	0.825	0.805	0.805
EL (mW), median (IQR)	PA	1.06 (0.91–1.22)	1.27 (0.92–1.53)	1.85 (1.39–2.95)	**0.019**	0.296	**0.016**	0.138
EL (mW), median (IQR)	TA	5 (3.25–5.7)	7.7 (5.25–9.9)	8.8 (6.8–14.55)	**0.009**	0.114	**0.007**	0.201
PWV (m/s), median (IQR)	PA	2.51 (2.21–2.72)	3.04 (2.55–4.06)	2.14 (1.6–7.49)	0.640	0.644	0.644	0.644
PWV (m/s), median (IQR)	TA	7.82 (6.56–8.55)	9.27 (8.20–9.91)	9.35 (8.18–10.32)	0.046	0.060	0.060	0.843
WSS (Pa), mean (SD)	AV	0.47 (0.17)	0.46 (0.20)	0.50 (0.18)	0.712	0.758	0.758	0.758
WSS (Pa), median (IQR)	PAA	0.44 (0.34–0.46)	0.29 (0.28–0.37)	0.46 (0.41–0.50)	0.070	0.167	0.497	0.077
WSS (Pa), mean (SD)	DAA	0.43 (0.19)	0.3 (0.13)	0.46 (0.14)	0.038	0.080	0.608	0.050
WSS (Pa), mean (SD)	BDA	0.58 (0.24)	0.53 (0.12)	0.45 (0.18)	0.279	0.758	0.344	0.344
WSS (Pa), median (IQR)	DA	0.53 (0.37–0.60)	0.47 (0.45–0.49)	0.38 (0.35–0.47)	0.155	0.791	0.192	0.192

Mean and SD are for normally distributed factors and median and IQR are for factors with no normal distribution.

Bold numbers delineate significant differences. AV: aortic valve; BDA: begin of the descending aorta; DA: descending aorta; DAA: distal ascending aorta; DAH: decellularized aortic homografts; EL: energy loss; IQR: interquartile range; MV: maximum velocity; PA: proximal aorta; PAA: proximal ascending aorta; PWV: pulse wave velocity; SD: standard deviation; TA: thoracic aorta; VSARR: valve-sparing aortic root replacement; WSS: wall shear stress.

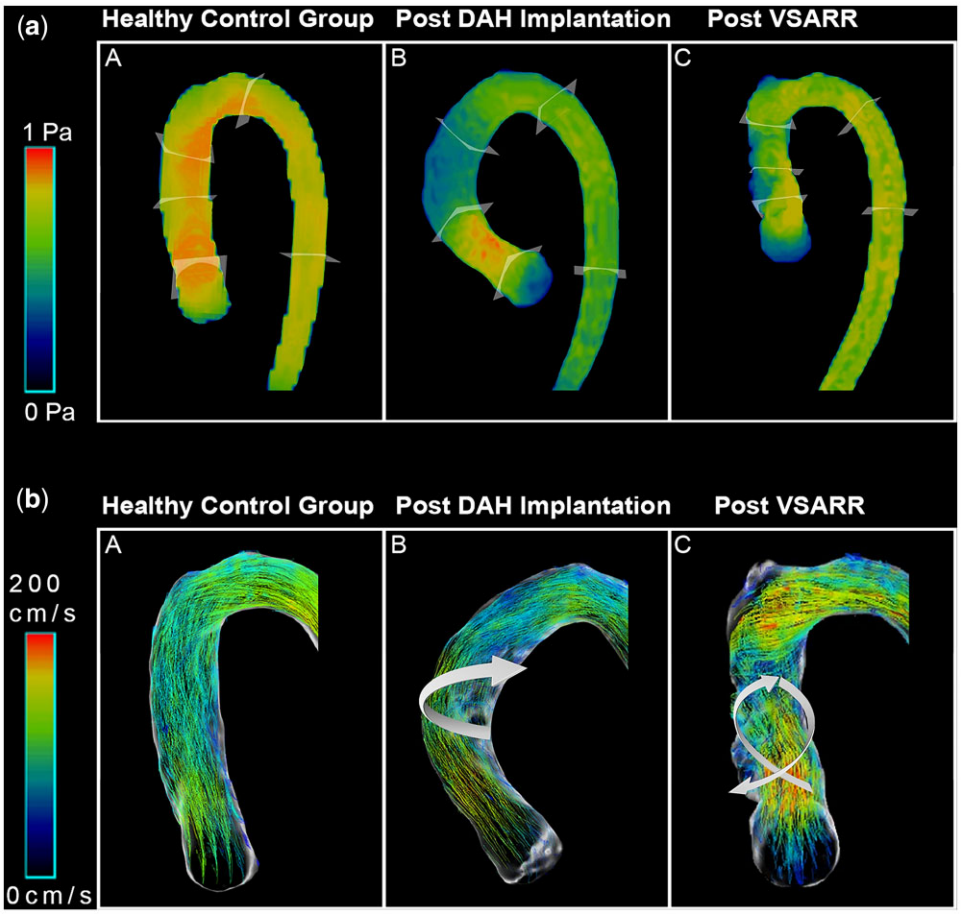

Figure 2: (**a**) Visualization of the wall shear stress in the whole thoracic aorta: A—healthy control, B—patient after decellularized aortic homograft implantation, and C—patient after valve-sparing aortic root replacement. (**b**) Demonstration of the secondary blood flow patterns using pathlines (i.e. trajectories of individual particles). Helical flow patterns were defined as helix in which the blood moves spirally in the main flow direction (B). Vortical flow is characterized with antegrade and retrograde flow with blood flow deviating from main direction (C).

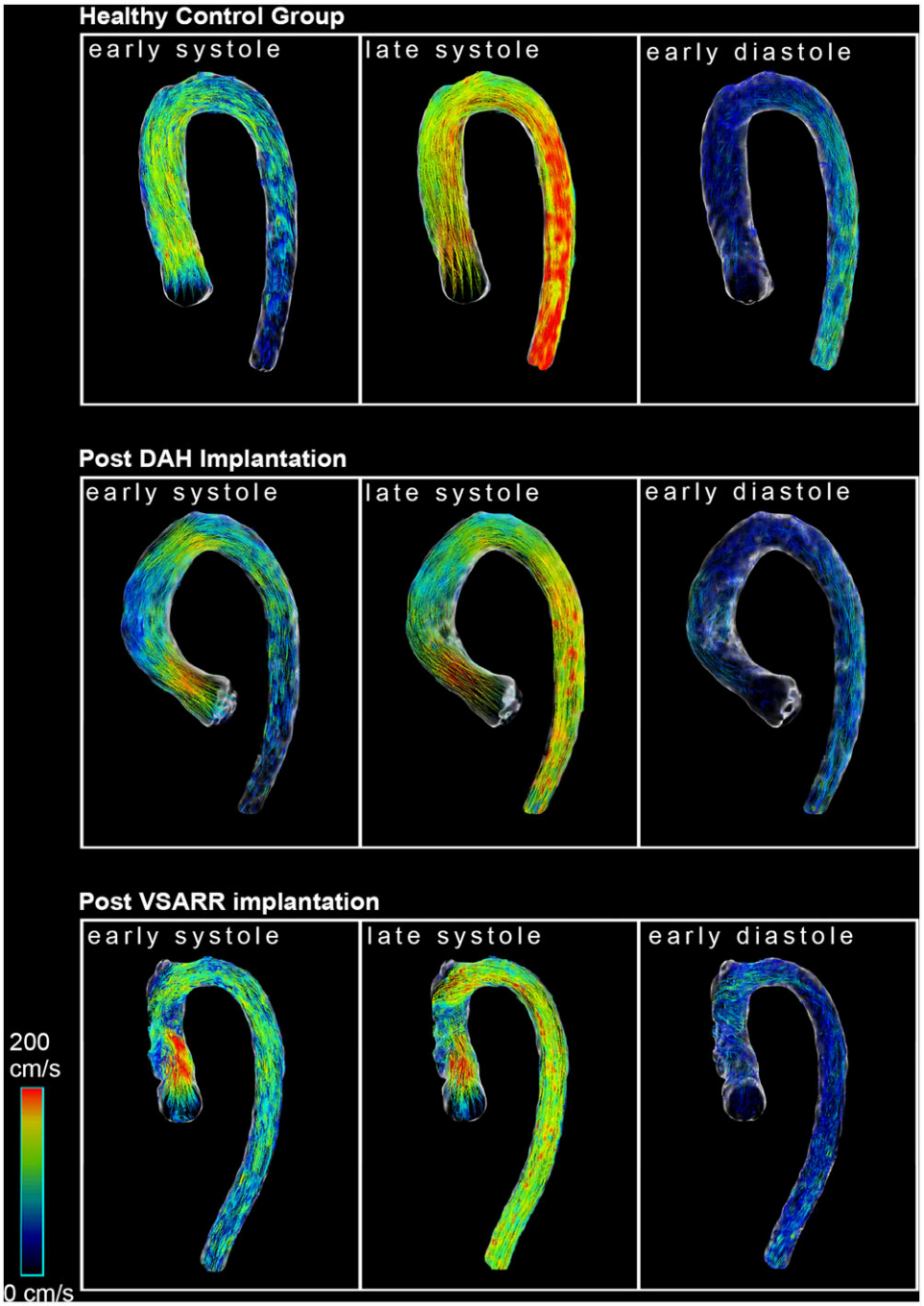

Figure 3: Visualization of the blood flow using particle traces (streamlines) in the whole thoracic aorta at different time points of the cardiac cycle: early systole, late systole, early diastole.

while there were no significant differences at the level of the aortic valve and at the level of descending aorta (Table 3 and Figs. 2b and 3).

DISCUSSION

In this study, we characterized postoperative haemodynamics following aortic root replacement using long DAH in comparison with a healthy control group and with patients who had undergone VSARR. The results show near normal data for flow velocity, pulse wave velocity, wall shear stress and EL in DAH when compared with healthy controls.

Our understanding of these results is that extended aortic root replacement using DAH fulfils the expectation of a near normal physiology, regarding flow dynamics, at least in the early postoperative phase. The results are also comparable with those for VSARR, the currently considered best option in aortic root dilatation for young patients. We are aware that VSARR is generally performed in a different patient sub-cohort than DAH, in which patients with smaller aortic rings and stenosis predominate. However, the only other option for young patients requiring

Table 3: Flow patterns in all 3 cohorts (healthy controls, decellularized aortic homografts, valve-sparing aortic root replacement)

Location	Variable (flow patterns)	Control ($n = 11$), median (IQR)	DAH ($n = 11$), median (IQR)	VSARR ($n = 11$), median (IQR)	*P*-omnibus	Control versus DAH, *P*-value	Control versus VSARR, *P*-value	DAH versus VSARR, *P*-value
Aortic valve	Eccentricity	0 (0)	0 (0)	0 (0)	0.999	0.999	0.999	0.999
	Helicity	0 (0)	0.27 (0.65)	0 (0)	0.127	0.700	0.999	0.700
	Vorticity	0 (0)	0.36 (0.67)	0 (0)	0.041	0.413	0.999	0.413
Proximal ascending aorta	Eccentricity	0 (0–0.5)	1 (0.5–1.0)	0 (0–0.5)	0.046	0.106	0.877	0.106
	Helicity	0 (0)	1 (1.0–2.0)	1 (0–1.0)	0.001	**0.001**	0.149	**0.045**
	Vorticity	0 (0–0.5)	1 (1–2)	0 (0–1)	0.009	**0.019**	0.434	0.079
Distal ascending aorta	Eccentricity	0 (0)	1 (1–2)	1 (0–1)	0.001	**0.001**	0.123	**0.045**
	Helicity	0 (0)	1 (1–2)	0 (0–1)	0.001	**0.004**	0.175	0.096
	Vorticity	0 (0)	1 (1–2)	0 (0–0)	0.001	**0.002**	0.537	**0.008**
Begin of the descending aorta	Eccentricity	0 (0)	0.18 (0.4)	0 (0)	0.127	0.700	0.999	0.700
	Helicity	0 (0)	0 (0)	0 (0)	0.999	0.999	0.999	0.999
	Vorticity	0 (0)	0.18 (0.6)	0 (0)	0.368	0.999	0.999	0.999
Descending aorta	Eccentricity	0 (0)	0.27 (0.47)	0 (0)	0.041	0.413	0.999	0.413
	Helicity	0 (0)	0.36 (0.67)	0 (0)	0.041	0.413	0.999	0.413
	Vorticity	0 (0)	0.36 (0.80)	0 (0)	0.127	0.700	0.999	0.700

Bold numbers delineate significant differences. DAH: decellularized aortic homografts; IQR: interquartile range; VSARR: valve-sparing aortic root replacement.

aortic valve replacement with secondary dilated aortopathy is mechanical valve replacement in combination with a prosthetic replacement for the aorta ascendens. As in VSARR, the use of prosthetic material will inevitably lead to increased stiffness and increased EL in the ascending aorta, both of which are reported as strong predictive markers for cardiovascular events, including all-cause mortality, in a multi-ethnic population free of overt cardiovascular disease in the MESA population [5, 11].

Another important aspect is the configuration of the aorta ascendens after repair. Straight vascular prostheses, as normally used in VSARR, may induce more flow disturbance than the physiological shape of a long DAH [26].

Flow characteristics after DAH, however, showed higher rates for helices and vortices compared with controls. This has also been reported for autograft replacement in Ross procedure patients by von Knobelsdorf-Brenkenhoff *et al.* [24] and, in our view, is related to the fact that DAH were predominantly implanted in patients with severe aortic stenosis, who had undergone more previous LVOT procedures and more previous cardiac interventions in general. We hypothesize that flow directions might be altered in DAH patients by a different left ventricular geometry due to pre-existing anatomical conditions or previous LVOT operations. Unfortunately, we had no access to whole-heart 4D-flow CMR, which would have been very helpful to clarify this hypothesis. The question is whether this level of pathological flow patterns in DAH will translate into reduced long-term durability [3]. Flow displacement and wall shear stress have been described as important factors leading to dilatation and dissection of the ascending aorta and therefore will have to be assessed regularly in the follow-up of our DAH patients [27, 28].

The longest follow-up in this cohort is currently 12 years, and no dilatation of DAH has been observed. We recently have shown that DAH can elicit a highly individual immune response through preformed antibody binding [29]. In paediatric patients, we have demonstrated less favourable long-term results than in adult patients after DAH implantation and it appears that the more active immune system in children may cause a subclinical immune response ultimately leading to an alteration in the otherwise good elastic properties, which we have demonstrated with the current analysis.

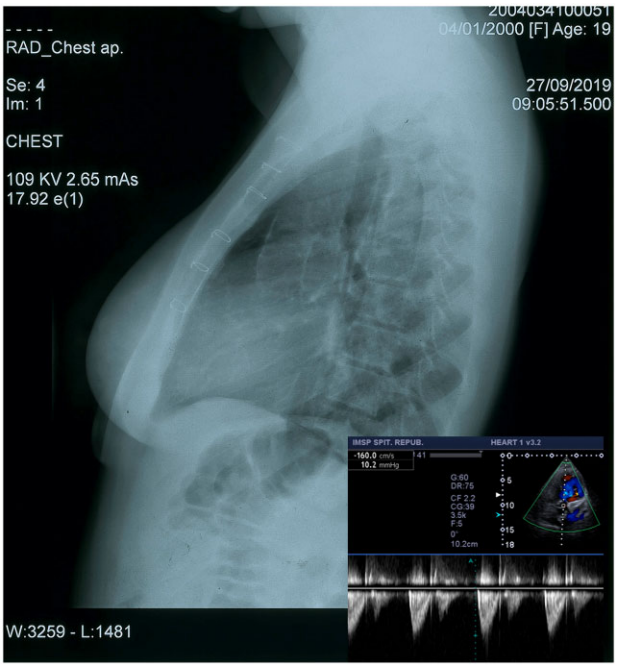

Figure 4: X-ray of a 19-year-old female patient 11 years postimplantation of a long decellularized aortic homograft. The implanted homograft, which showed excellent aortic valve function with normal flow velocity and no regurgitation, can be easily differentiated by intramural calcification as an indirect evidence for an ongoing immune response against the graft.

Figure 4 shows the X-ray of a 19-year-old female patient 11 years after the implantation of a long DAH. The implanted homograft, which showed excellent aortic valve function with normal flow velocity and no regurgitation, can be easily differentiated by intramural calcification as an indirect evidence for an ongoing immune response towards the graft. This underlines the need for long-term follow-up in any new cardiovascular device

on a biological basis. Consequently, we have planned serial follow-up of the patient cohorts described in this study. DAH patients will be also followed within the ARISE study and the ARISE Registry to provide information about the long-term behaviour of DAH. Ideally, a randomized comparison to the Ross procedure would be performed in addition [30].

Future analysis will also have to assess the complexity of redo procedures following DAH implantation. Our initial experience in this type of redo aortic root surgery has so far shown less complexity and better outcomes due to reduced calcification. In a recently published paediatric multicentre study, there were no mortalities in 7 DAH explantations, 4 redo DAH, 2 mechanical AVR and 1 HTx [31].

The availability of donated homografts is another important aspect regarding the potential use of DAH for extended aortic valve replacement. To overcome this limitation we, and others, have started research on the use of decellularized xenogenic heart valves from genetically modified animals [29].

Limitations

The main limitations of this study are the limited number of participants, a relatively short follow-up period and the lack of longitudinal data. The strengths of the study are the good comparability of the 3 study groups with respect to myocardial function, cardiac output data and the time after surgical procedure.

Another limitation is the lack of a control group with mechanical aortic valve replacement and prosthetic substitution of the ascending aorta, who matched the characteristics of our DAH cohort.

Due to the required scan duration, 4D-flow CMR was focused on the thoracic aorta. Therefore, we were not able to analyse LVOT haemodynamics with respect to helicity and vorticity, with this method. A 4D-stress CMR to test DAH flow conditions during exercise would also have been very interesting. With the availability of faster 4D-flow CMR sequences, we are planning 4D-flow CMR of the heart and the great vessels as a 'one-stop-shop' solution for the planned longitudinal follow-up of the DAH cohort.

We included only male study subjects. Female patients were intentionally excluded for a more uniform study cohort, especially with regard to body size and cardiac output parameters. Sex-specific post-surgical alterations in fluid dynamics in the ascending aorta therefore cannot be ruled out but, in our view, are unlikely.

CONCLUSION

Decellularized long aortic homografts exhibit near normal haemodynamic parameters when assessed by 4D-flow CMR 2.56 ± 2 years postoperatively.

In patients with aortic valve pathology and associated dilatation of the aortic root and ascending aorta, in which preservation of the aortic valve is not feasible, extended aortic valve replacement using long DAH is an additional surgical option.

SUPPLEMENTARY MATERIAL

Supplementary material is available at *EJCTS* online.

Funding

This study was supported by a grant from the European Union's HORIZON 2020 Programme under Grant Agreement No. 643597 (www.arise-clinicaltrial.eu).

Conflict of interest: Axel Haverich holds shares in Corlife oHG, the company providing the service of processing decellularized allografts used in this study.

Data Availability Statement

The data underlying this article will be shared on reasonable request to the corresponding author.

Author contributions

Tomislav Cvitkovic: Conceptualization; Data curation; Formal analysis; Investigation; Methodology; Writing—original draft. **Dmitry Bobylev:** Data curation; Investigation; Methodology; Writing—original draft. **Alexander Horke:** Data curation; Methodology; Supervision; Writing—review & editing. **Murat Avsar:** Investigation; Methodology; Supervision; Writing—review & editing. **Philipp Beerbaum:** Investigation; Methodology; Supervision; Writing—review & editing. **Andreas Martens:** Conceptualization; Resources; Writing—review & editing. **Dietmar Böthig:** Formal analysis; Software; Visualization; Writing—review & editing. **Elena Petenà:** Data curation; Resources; Supervision; Writing—review & editing. **Marcel Gutberlet:** Conceptualization; Data curation; Resources; Supervision. **Frerk Hinnerk Beyer:** Conceptualization; Data curation; Resources; Supervision. **Frank Wacker:** Data curation; Resources; Supervision; Writing—review & editing. **Serghei Cebotari:** Methodology; Resources. **Axel Haverich:** Data curation; Resources; Supervision; Writing—review & editing. **Jens Vogel-Claussen:** Conceptualization; Project administration; Resources; Supervision; Writing—review & editing. **Samir Sarikouch:** Conceptualization; Funding acquisition; Project administration; Supervision; Writing—review & editing. **Christoph Czerner:** Conceptualization; Formal analysis; Methodology; Project administration; Resources; Supervision; Writing—original draft.

Reviewer information

European Journal of Cardio-Thoracic Surgery thanks Julia Dumfarth, Sven Peterss, Filippo Piacentino and the other, anonymous reviewer(s) for their contribution to the peer review process of this article.

REFERENCES

[1] Zhao DF, Seco M, Wu JJ, Edelman JB, Wilson MK, Vallely MP *et al.* Mechanical versus bioprosthetic aortic valve replacement in middle-aged adults: a systematic review and meta-analysis. Ann Thorac Surg 2016;102:315–27.

[2] Shrestha ML, Beckmann E, Abd Alhadi F, Krueger H, Meyer-Bockenkamp F, Bertele S *et al.* Elective David I procedure has excellent long-term results: 20-year single-center experience. Ann Thorac Surg 2018;105:731–8.

[3] Tudorache I, Horke A, Cebotari S, Sarikouch S, Boethig D, Breymann T *et al.* Decellularized aortic homografts for aortic valve and aorta ascendens replacement. Eur J Cardiothorac Surg 2016;50:89–97.

[4] Sekaran NK, Crowley AL, de Souza FR, Resende ES, Rao SV. The role for cardiovascular remodeling in cardiovascular outcomes. Curr Atheroscler Rep 2017;19:23.

[5] Noda C, Ambale Venkatesh B, Ohyama Y, Liu CY, Chamera E, Redheuil A *et al.* Reproducibility of functional aortic analysis using magnetic resonance imaging: the MESA. Eur Heart J Cardiovasc Imaging 2016;17:909–17.

[6] Hope MD, Hope TA, Crook SE, Ordovas KG, Urbania TH, Alley MT *et al.* 4D flow CMR in assessment of valve-related ascending aortic disease. JACC Cardiovasc Imaging 2011;4:781–7.

[7] Bissell MM, Hess AT, Biasiolli L, Glaze SJ, Loudon M, Pitcher A *et al.* Aortic dilation in bicuspid aortic valve disease: flow pattern is a major

contributor and differs with valve fusion type. Circ Cardiovascular Imaging 2013;6:499–507.
[8] Markl M, Frydrychowicz A, Kozerke S, Hope M, Wieben O. 4D flow MRI. J Magn Reson Imaging 2012;36:1015–36.
[9] Markl M, Draney MT, Miller DC, Levin JM, Williamson EE, Pelc NJ *et al.* Time-resolved three-dimensional magnetic resonance velocity mapping of aortic flow in healthy volunteers and patients after valve-sparing aortic root replacement. J Thorac Cardiovasc Surg 2005;130:456–63.
[10] Kvitting JP, Ebbers T, Wigstrom L, Engvall J, Olin CL, Bolger AF. Flow patterns in the aortic root and the aorta studied with time-resolved, 3-dimensional, phase-contrast magnetic resonance imaging: implications for aortic valve-sparing surgery. J Thorac Cardiovasc Surg 2004;127:1602–7.
[11] Redheuil A, Wu CO, Kachenoura N, Ohyama Y, Yan RT, Bertoni AG *et al.* Proximal aortic distensibility is an independent predictor of all-cause mortality and incident CV events: the MESA study. J Am Coll Cardiol 2014;64:2619–29.
[12] Murgo JP, Westerhof N, Giolma JP, Altobelli SA. Aortic input impedance in normal man: relationship to pressure wave forms. Circulation 1980; 62:105–16.
[13] Vlachopoulos C, Aznaouridis K, Stefanadis C. Prediction of cardiovascular events and all-cause mortality with arterial stiffness: a systematic review and meta-analysis. J Am Coll Cardiol 2010;55:1318–27.
[14] Laurent S, Boutouyrie P, Asmar R, Gautier I, Laloux B, Guize L *et al.* Aortic stiffness is an independent predictor of all-cause and cardiovascular mortality in hypertensive patients. Hypertension 2001;37:1236–41.
[15] Ben-Shlomo Y, Spears M, Boustred C, May M, Anderson SG, Benjamin EJ *et al.* Aortic pulse wave velocity improves cardiovascular event prediction: an individual participant meta-analysis of prospective observational data from 17,635 subjects. J Am Coll Cardiol 2014;63:636–46.
[16] Oechtering TH, Sieren MM, Hunold P, Hennemuth A, Huellebrand M, Scharfschwerdt M *et al.* Time-resolved 3-dimensional magnetic resonance phase contrast imaging (4D Flow MRI) reveals altered blood flow patterns in the ascending aorta of patients with valve-sparing aortic root replacement. J Thorac Cardiovasc Surg 2020;159:798–810 e1.
[17] Markl M, Chan FP, Alley MT, Wedding KL, Draney MT, Elkins CJ *et al.* Time-resolved three-dimensional phase-contrast MRI. J Magn Reson Imaging 2003;17:499–506.
[18] Reiter U, Reiter G, Fuchsjager M. MR phase-contrast imaging in pulmonary hypertension. Br J Radiol 2016;89:20150995.
[19] Markl M, Wallis W, Brendecke S, Simon J, Frydrychowicz A, Harloff A. Estimation of global aortic pulse wave velocity by flow-sensitive 4D MRI. Magn Reson Med 2010;63:1575–82.
[20] Wentland AL, Grist TM, Wieben O. Review of MRI-based measurements of pulse wave velocity: a biomarker of arterial stiffness. Cardiovasc Diagn Ther 2014;4:193–206.
[21] Dyverfeldt P, Ebbers T, Lanne T. Pulse wave velocity with 4D flow MRI: systematic differences and age-related regional vascular stiffness. Magn Reson Imaging 2014;32:1266–71.
[22] Stalder AF, Russe MF, Frydrychowicz A, Bock J, Hennig J, Markl M. Quantitative 2D and 3D phase contrast MRI: optimized analysis of blood flow and vessel wall parameters. Magn Reson Med 2008;60: 1218–31.
[23] Barker AJ, van Ooij P, Bandi K, Garcia J, Albaghdadi M, McCarthy P *et al.* Viscous energy loss in the presence of abnormal aortic flow. Magn Reson Med 2014;72:620–8.
[24] von Knobelsdorff-Brenkenhoff F, Trauzeddel RF, Barker AJ, Gruettner H, Markl M, Schulz-Menger J. Blood flow characteristics in the ascending aorta after aortic valve replacement–a pilot study using 4D-flow MRI. Int J Cardiol 2014;170:426–33.
[25] Geiger J, Markl M, Herzer L, Hirtler D, Loeffelbein F, Stiller B *et al.* Aortic flow patterns in patients with Marfan syndrome assessed by flow-sensitive four-dimensional MRI. J Magn Reson Imaging 2012;35:594–600.
[26] Sieren MM, Balks Mf Schlueter Jk Wegner F, Huellebrand M, Scharfschwerdt M *et al.* Comprehensive analysis of haemodynamics in patients with physiologically curved prostheses of the ascending aorta. Eur J Cardiothorac Surg 2021;ezab352.
[27] Korpela T, Kauhanen SP, Kariniemi E, Saari P, Liimatainen T, Jaakkola P *et al.* Flow displacement and decreased wall shear stress might be associated with the growth rate of an ascending aortic dilatation. Eur J Cardiothorac Surg 2021;ezab352.
[28] Hohri Y, Numata S, Itatani K, Kanda K, Yamazaki S, Inoue T *et al.* Prediction for future occurrence of type A aortic dissection using computational fluid dynamics. Eur J Cardiothorac Surg 2021;60:384–91.
[29] Ebken J, Mester N, Smart I, Ramm R, Goecke T, Jashari R *et al.* Residual immune response towards decellularized homografts may be highly individual. Eur J Cardiothorac Surg 2021;59:773–82.
[30] Horke A, Tudorache I, Laufer G, Andreas M, Pomar JL, Pereda D *et al.* Early results from a prospective, single-arm European trial on decellularized allografts for aortic valve replacement: the ARISE study and ARISE Registry data. Eur J Cardiothorac Surg 2020;58: 1045–53.
[31] Horke A, Bobylev D, Avsar M, Meyns B, Rega F, Hazekamp M *et al.* Paediatric aortic valve replacement using decellularized allografts. Eur J Cardiothorac Surg 2020;58:817–24.